INVESTIGATION AND COMPARISON THE MECHANICAL BEHAVIOR OF 30SN70PB AND SAC305 AS LEAD AND LEAD-FREE SOLDER ALLOYS IN COMPRESSION PROCESSES

[1]ALAA HASAN ALIALSHAMMARI, [2]INTESSAR A. HADI

[1,2]Department of Materials Engineering Machines & Equipment Eng. Department
University of Technology, Baghdad – Iraq University of Technology, Baghdad – Iraq
E-mail: dr_alaahassan@yahoo.com, in.issa@yahoo.com

Abstract- Mechanical behavior of each of SAC305 and 30Sn70Pb as lead-free and lead-based solder alloys was investigated and compared; more than 60spherical balls samples were compressed to identify statistical variability in the properties in each alloy. Isothermal aging was done to study and compare the aging effect on the microstructure and properties.
The results showed significant elastic and plastic anisotropy of tin phase in lead- free alloys and micro structural changes and stability under isothermal aging processes.

Keywords- Tin Anisotropy Behavior, Lead-Free Solder, And Composite Solder.

I. INTRODUCTION

Due to potential hazards associated with the toxicity of lead affords has been taken to use Lead -free solders specially in electronic assembly industry and eliminate or replace the tin in consumer products. So, Tin based solders have become the dominant choice for electronic industries.
Previous studies focus on the tin anisotropy and the effect of this material characteristic on mechanical properties of lead-free solder joints and their behavior during mechanical deformation and thermal processes [2, 4, 7]. There are very few investigations on the statistical variation of mechanical properties of as fabricated lead-free solder balls [6, 3]. Therefore Further investigations are required to be conducted to provide more insights into the effects of processing parameters and also alloy compositions on the mechanical properties of different solders. The focus of this study is to provide enough statistical data to be able to compare the joint scale mechanical behavior of the lead free solders and different lead based solders to gain insights into the effect of anisotropy associated with the coarse grain microstructure of lead free solders with isotropic properties of lead based solders.
Recently, there have been many investigations regarding the mechanical properties of the lead-free solders [1, 13]. However there is lack of understanding about the mechanical properties of these alloys. The existing information in the literature are from a different fabrication and testing process which causes variation in microstructures and mechanical properties associated with these microstructures [8]. Therefore in order to develop a reliable model to predict the deformation behavior of lead-free solders, a comprehensive understanding of mechanical properties is required.
The isotropy associated with the polycrystalline microstructure of lead based solder as well as the interaction between different phases (Pb as a soft phase and tin as a hard phase) traditional modeling procedures based upon the isotropic hardening and creep models can be quite efficient in prediction of damage in electronic packages specially in the thermal cycling loading conditions [7,9,10]. However use of these methods for prediction of the location of failure is not promising in lead free solders.
Many works focus on the variability of solder balls of different alloys and their effect on manufacturing electronic system. Additional work ought to be done to improve the scientific understanding variable properties of solder balls for different alloys so the motives of the present study are to give more understanding how the different balls sizes and Sn elastic and Plastic anisotropy phenomena effect on the strength and ratability of solder joint of manufactured electron system and must be taken into consideration by manufacturer and supplier.

II. CRYSTAL PLASTICITY FORMULATION

A velocity gradient in plastic deformation in the material coordinate system can be decomposed into a rate of deformation and a spin tensor as:

$$L^P = D^P + W^P \quad (1)$$

An elasto-plastic problem is usually defined as a constrained optimization problem aimed at finding the optimum stress tensor and internal variables for a given strain increment. In such a problem, the objective function is defined based on the principle of maximum dissipation and is made of terms describing the incremental release of elastic strain energy and the dissipation due to the incremental plastic work and the constraint is the yield function

$$\left(\sigma_{j+1}, q_{j+1}\right) = \begin{cases} \text{Min}[l(x) = \left(\sigma_{j+1}^{trial} - \sum\right) : C^{-1} : \left(\sigma_{j+1}^{trial} - \sum\right) + \left(q - q_j\right) : E^{-1} : \left(q - q_j\right)] \\ \text{Subjected to : } f(\sum, q) \le 0 \end{cases} \quad (2)$$

where $\sum$ is the design variable (stress tensor) to be found, q is a vector containing the internal variables such as strain hardening and kinematic hardening

variables to be found, C is the material stiffness matrix, f(∑, q) is the yield function, and E is the so-called matrix of generalized hardening moduli. One of the solutions to the above problem is the following equation for the plastic rate of deformation

$$D^p = \lambda \frac{\partial f(\sigma,q)}{\partial \sigma} \quad (3)$$

In a crystal plasticity problem, the deformation is defined by several yield surfaces, and the number of yield functions depends on the number of slip systems in a crystal. Assuming the validity of the Schmidt law for the plastic deformation of a single crystal, then for any slip system a yield function can be defined as:

$$f_\alpha(\sigma, q) = \frac{|\sigma : P^\alpha|}{\tau_y^\alpha} - 1 \quad (4)$$

the constraints of problem (2) can be combined and replaced by an equivalent single constraint defined as:

$$f(\sigma, q) = \frac{1}{\rho} \ln\left[\sum_{i=1}^{m} \exp\left[\left(\rho \frac{|\sigma : P^\alpha|}{\tau_y^\alpha} - 1\right)\right]\right] \quad (5)$$

where τ_y^α is the critical shear stress on slip plane α, and P^α is a matrix showing the orientation of a slip system and is defined by:

P^α is the symmetric part of the Schmid tensor, I^α, describing the orientation of a slip system, defined as:

$$P^\alpha = \frac{1}{2}[(I^\alpha) + (I^\alpha)^T] = \frac{1}{2}(m^\alpha \otimes n^\alpha + (m^\alpha \otimes n^\alpha)^T) \quad (6)$$

where n^α is a unit normal to the slip plane, and m^α is a unit vector denoting the slip direction.

The plastic deformation matrix can be expressed as

$$D^p = \sum_{\alpha=1}^{N} \dot{\gamma}^\alpha P^\alpha \quad (7)$$

Where $\dot{\gamma}$ are the slip rates.

And spin tensor, which represents the material axis rotation, can be expressed as:

$$\Omega^p = \sum_{\alpha=1}^{N} \dot{\gamma}^\alpha w^\alpha \quad (8)$$

Where w^α matrix is the anti-symmetric part of I^α, defined as:

$$w^\alpha = \frac{1}{2}(m^\alpha \otimes n^\alpha - (m^\alpha \otimes n^\alpha)^T) \quad (9)$$

Using equation 3,5 and 7, it can be shown that during the plastic deformation of a single crystal the slip rate on any slip system could be expressed by, [15]:

$$\dot{\gamma}^\alpha = \lambda \frac{\frac{\mathrm{sgn}(\sigma:P^\alpha)}{\tau_y^\alpha} \exp\left[\left(\frac{\rho}{m} \frac{|\sigma:P^\alpha|}{\tau_y^\alpha} - 1\right)\right]}{m \sum_{\beta=1}^{N} \exp\left[\left(\frac{\rho}{m} \frac{|\sigma:P^\alpha|}{\tau_y^\alpha} - 1\right)\right]} \quad (10)$$

Where m and ρ are material parameters that control the shape of the single-crystal yield surface, and been shown to have a direct relationship with the stacking fault energy (SFE) of the material as following:

$$\rho = \frac{5\Gamma}{Gb} \times 10^{-3} \quad (11)$$

Where Γ is the SFE of the material, G is the shear modulus, and b is the magnitude of Burgers vector. For most materials m = 1 Parameter λ is a Lagrange multiplier which has been shown to be a measure of the rate of plastic work in a crystal,

The generalized Schmidt factor can be found for each slip system α by finding the scalar product of the normalized stress tensor (using the Frobenious norm) and the Schmidt matrix.

In order to define the resistance against the shear, Hill, [16], andAsaro and Needleman, [17], proposed the following formulation:

$$\dot{\tau}^\alpha = \sum_{\beta=1}^{N} h^{\alpha\beta} |\dot{\gamma}^\beta| \quad (12)$$

Where $|\dot{\gamma}^\beta|$ is the plastic slip rate on the active slip system β, and $h^{\alpha\beta}$ are the components of the hardening matrix $h^{\alpha\alpha}$ are known as the self-hardening moduli while $h^{\alpha\beta}$ for $\alpha \neq \beta$ are known as the latent-hardening moduli. Hutchison, [18], proposed the following model for evolution of the components of hardening matrix

$$h^{\alpha\beta} = h^\beta [q + (1 - q)\delta^{\alpha\beta}] \quad (13)$$

Here q is the so-called latent-hardening ratio, which is the hardening on a secondary slip system caused by slip on a primary slip system (KapoorandNemat-Nasser, [19]) and can be measured by the ratio of the latent-hardening rate to the self-hardening rate of a slip system with typical values in the range of $1 < q < 1.4$. The parameter q can be considered as 1 for coplanar slip systems and 1.4 for non-coplanar slip systems. There are different kinds of hardening models presented by researchers for the evolution of h^β (so-called self-hardening). One of the most well-known formulations is:

$$h^\beta = h_0 \left|1 - \frac{\tau_y^\beta}{\tau_s}\right|^a \mathrm{sgn}\left(1 - \frac{\tau_y^\beta}{\tau_s}\right) \quad (14)$$

where h_0, a, and τ_s are slip system hardening parameters, which are considered to be identical for all slip systems, h_0 denotes the initial hardening rate, τ_s the saturation value of the slip resistance, and a the exponent describing the shape of the stress-strain yield function. These parameters can be obtained by fitting the model to experimental data.

III. EXPERIMENTAL METHODS

More than 60 balls that were (420-600) microns in diameter of Tin-Lead and Lead –Free solder alloys(Table1) [20], were studied and evaluated. Each ball was individually compressed, to compare the load-displacement deformation behavior of each material. The loading stage with one ball is illustrated in Figure 1.

3-1. Balls Compression Process:

The compression process was accomplished using a Rheometric Solids Analyzer instrument model RSS 111 (Figure 1) at room temperature.

The compression test methodology was used to obtain the time-dependents material response of

compression of a ball shaped sample. Each solder ball had a spherical diameter of (420-600)micron , this range of balls diameters was found from loading – unloading processes for each ball solder materials.

Balls were put in place on the loading platens, and centered approximately close to the loading axis. Then the instrument was calibrated to maximum cap of 600 microns (according to the maximum balls diameter range) and for each ball compression process , the instrument is setting to the reference point command cap to 600 micron , then starting compression test , loading was applied when the loading platen was lowered with simultaneous data acquisition at a rate of 0.01mm/s until a particular displacement was reached, the particular displacement was be fixed in instrument control zone by time interval of 15 sec and a rate of 0.01mm/s . Because each ball had a different diameter, the maximum strain imposed varied from sample to sample. The samples were loaded up to a given displacement of (150) microns. As each ball had a different diameter, the load reached at maximum load consequently had a displacement that varied loading was conducted to a different displacement.

3-2. Aging Processes:

To investigate the effect of grain size on the loading, some alloys were aged to 150 C for 170 hours in a Carbolite Temperature Control Oven, type 3508. The microstructure of selected balls before and after aging was investigated after polishing, (butthese balls were not deformed).

Aging experiments were performed by placing the solder balls into CARBOLITE Temperature Control Oven,Type (3508) at agingtemperature for 170 hours. Then the balls were slightly polished to remove the oxide layer resulting from to reveal the change in microstructure. Scanning electron micrographs of different balls weretaken before and after aging process to compare grain growth.

IV. RESULTS AND DISCUSSION

4-1.Compression test results:

During the compression processes various deformation behaviors occurred which represent the variation in mechanical property variability for different alloys. This clear in loading–unloading processes and in Maximum–Loading processes.

Figure (2) shows the loading –unloading curves of SAC305 alloy chosen from a batch of solder balls supplied by a manufacturer, during compression and unloading process. The load displacements data were shifted along the displacement axis until one of the datum points close to 0 displacements so that all of the curves would have a nearly common initial loading point, to assist comparison. Figure (3) for loading- maximum load, the difference in loading behavior can be more clearly observed. From the known initial and final displacement values, different original ball diameter between (426- 449)microns were identified and different deformation behaviors of each sample are apparent, particularly with regard to the loading slopes of each ball. Samples 13, 11, and 14 show representative value of relatively hard, soft, and in-between deformation behavior. From the load magnitude for these two samples at the same displacement, different load values vary by a factor of 25%.

Figures (4)and (5)show loading –unloading and maximum load deformation processes for 30Sn70Pb alloy respectively, variety in unloading slope for some samples according to different diameters of compressed balls, for the same reason, maximum load deformation processes shows large difference de formation interval nearly for same force comparing with others.

4-2. Aging Processes results:

Figures (6-13) show SEM Images for microstructure of different alloy Samples at room temperature and after aging processes at 150˚C for 170 hours. The optical and polarized images ofSAC305microstructure in Figure (6) shows alight region Sn-rich phase, $Ag_3\,Sn$participate particles, and small dark particles of Cu, while in Figure (7) reveals a crossed polarize picture of as received ball. Optical and polarized images in Figures (8) and (9)after aging process, Figure (8) shows significantly ball micro structural changes and its stability under is othermal aging condition and coarsening of Sn particles. In Figure (9) the polarized image shows three large regions with different colors (corresponding to no more than three main Sn grain orientations).

The distribution of Sn and Pb grains structure of tin-lead alloy 30Sn70Pb before aging is shown in Figures(10) and (11) , Sn grains with light color and Pb-rish with dark color.

microstructure of solder after aging process shown in Figures (12) and (13) with no scientifically Sn grains orientation.

4.3. Simulation Results

Simulation approach was done of solder materials SAC305 as a Lead-Free solder alloy and the second 30Sn70Pb as a Tin-lead based solder alloy to compare the deformation behavior for each solder.

The simulation approach results are represented by two Figures (14) and(15).According to the compression deformation results, the different behavior of each material during compression deformation and its effect on variable the properties of solder balls, which interpret the anisotropy grain behavior forSAC305, as shown in Figures (2) and (3). Anisotropy is very strong in Sn and has large effect on the reliability , the fracture probability in lead – based solder alloy is different from that in Lead-Free solder alloys, mostly because of the anisotropy present in Tin phase [20]. That is clear in variety in

Loading –Unloading slope and also in the different amount of Maximum load for some ball during deformation.

This behavior is clear in the microstructure of SAC305 before and after aging. The orientation of grain illustrate very clear the anisotropy behavior of Sn grain Figures. (8) and (9) and also is illustrated in Simulation Figure (14).

When material is formed, the grains are usually distorted and elongated in one or more direction which makes the Martials Anisotropy. As the microstructure of solder coarsening during the aging process, it is necessary to investigate its influence on the mechanical properties of the solders.

The characterization of lead –Free solder, especially after isothermal aging, is very important in order to accurately predict there liability of solder balls, and the grain size and morphology have significant effect on the mechanical properties of sub-mm scale balls.

Optical micrographs show bright field image of as an received sample , while polarized micrographs reveal a crossed polarizer picture of solder ball, it can be seen that large region with different colors corresponding to main Sn grain orientation increase in aging samples.

The Simulation approach supported the experiments results for SAC305 and that is shown in Figure (14),the isotropic model is too far from the experimental results showing that isotropic hardening overestimates the hardening. The anisotropy of Sn grains in SAC305 lead-free solder alloy interpret the different behavior of deformation of balls and its effect on mechanical proprieties like Modulus of elasticity, Strength, and Reliability. Simulation results of compression tests for 30Sn70Pb in Figure (15) are showing that the isotropic model matches well with experimental data.

CONCLUSION

Compression deformation of different metals of tin-lead and lead-free solders and aging processes at 150 ˚C for 170 hours were done in order to get a comprehensive understanding the mechanical properties of the solders during deformation behavior and isothermal aging processes , and from the experimental and simulation results we can conclude the following :

1. Loading-unloading deformation processes give good understanding the variety if deformation behavior and its effect on mechanical properties and the relation of maximum load –displacement show clearly interrelation between the magnitude of elastic-plastic deformation with anisotropy phenomena of tin-rich lead-free solder alloys.
2. Aging processes at 150 ˚C for 170 hours is suitable for alloy aged –softened and this softening correlated with the growth of relatively large tin- rich crystals and the coercing of Sn particles.
3. CPFE model can solve the mechanical deformation behavior of materials under compression effect. For SAC305 as a lead-free solder the simulation results for compression test showing that since the plastic deformation occurs in a small region of the sample, the difference between differed orientations is observed in large deformation. As is highlighted, the isotropic model is too far from the experimental results showing that isotropic hardening overestimated the hardening.
   Simulation result for tin-lead solder 30Sn70Pb c compression matches the experimental data are interpreting the homogenous deformation behavior of 30Sn70Pb balls as a tin-lead solder and support its isotopic phenomenon.
4. The different specification of manufacturing balls as received like sizes and different deformation behavior give us scientifically effect on the mechanical properties which must be taken into consideration by manufacturer and suppliers.
5. The fact that the microstructure remains stable under isothermal aging conditions is beneficial for manufacturing operation when reflow of solder joints.
6. Further study can be done for other different materials to investigate tin anisotropy.
7. Investigation can be done by reflow same materials and testing as solder joints and compare with present results.

ACKNOWLEDGMENT

The Author presents thanks to Professor And ree Lee, Professor Farhang Pourboghrat, and Professor Tom Bieler for thier advices and reviewing. Many thanks to Dr. PayamDarbandi for his help in simulation process.

Table 1. Chemical Composition of Tin-lead and Lead-free solder

Chemical Composition	Melting Temperature ˚C	*Young's* Modulus GPa	UTS MPa
SAC305	217	54	36
30Sn70Pb	185	32	42.30

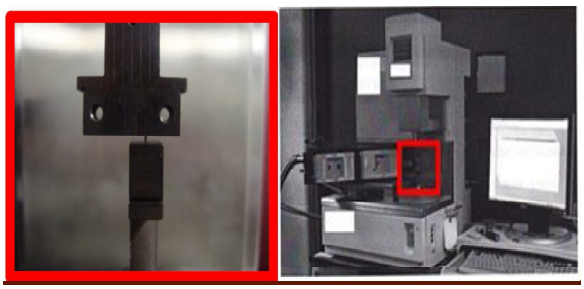


Figure 1. Ball compression fixture within Rheometric Solids Analyzer machine (Compliance 6.996E-05 mm/gm.)

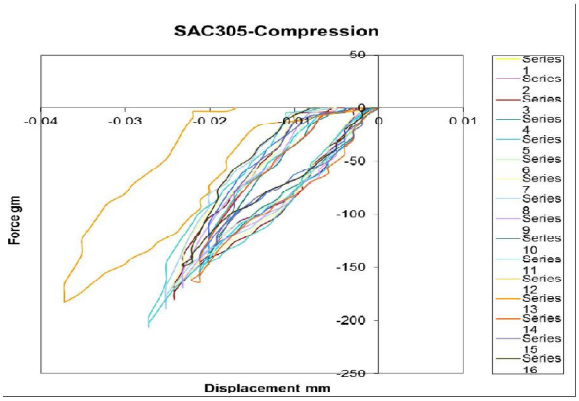


Figure (2) SAC305 Loading-Unloading

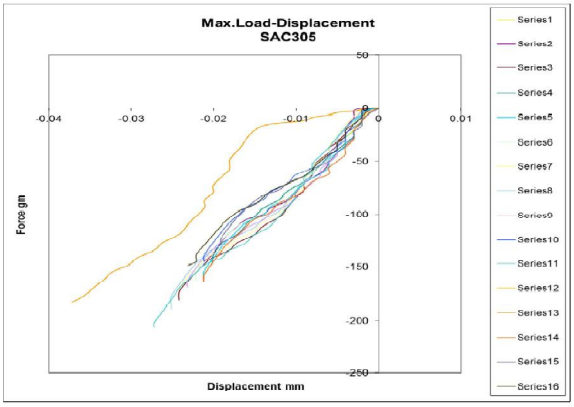


Figure (3) SAC305 Loading to maximum load

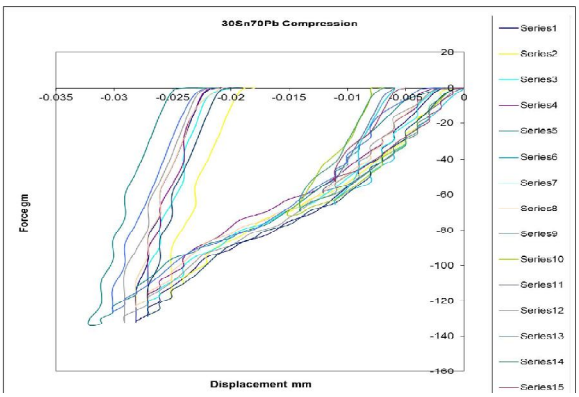


Figure (4) 30Sn70Pb Loading-Unloading

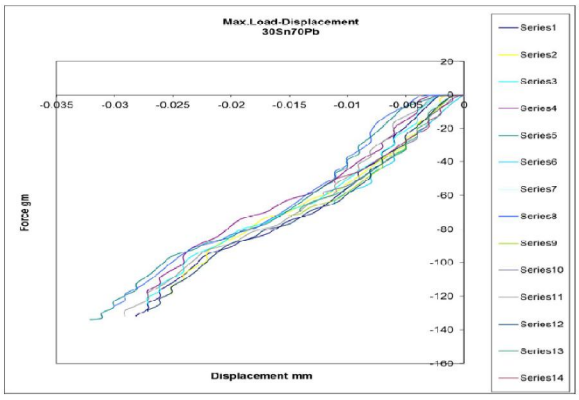


Figure (5) 30Sn70Pb loading to maximum load

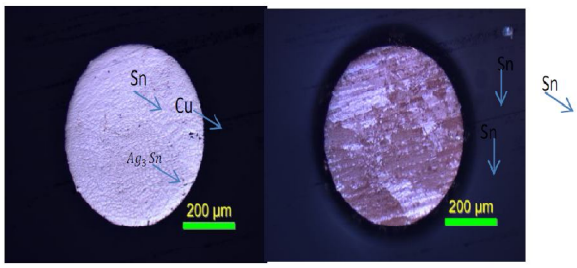


Figure (6) SAC305 micro structure Figure (7) SAC305 micro structure optical image before aging polarized image before aging

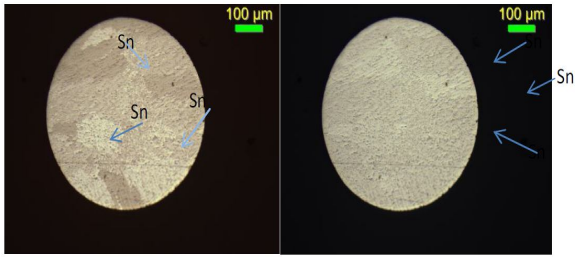


Figure (8) SAC305 microstructure Figure (9) SAC305 microstructure optical image after aging polarized image after aging

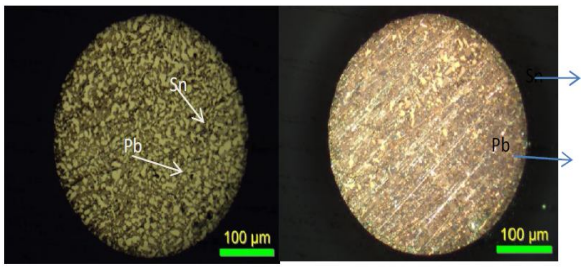


Figure (10) 30Sn70Pb microstructure Figure (11) 30Sn70Pb microstructure optical image before aging polarized image before aging

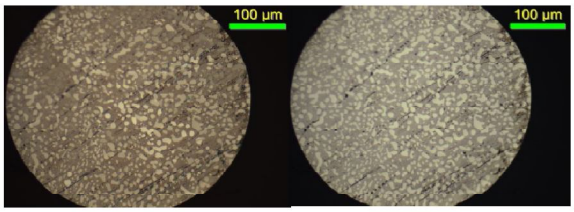


Figure (12) 30Sn70Pb microstructure Figure (13) 30Sn70 Pb microstructure polarized image after aging optical image after aging

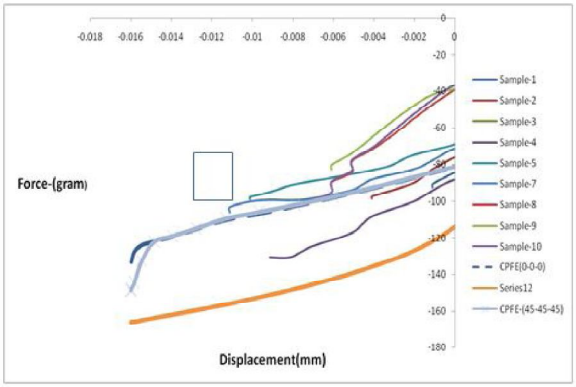


Figure (14) SAC305 Compression Simulation

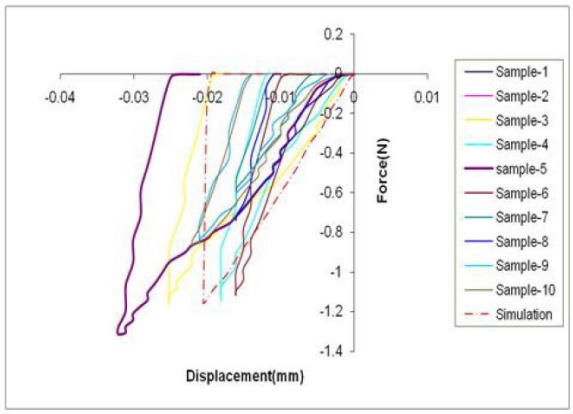


Figure (15) 30Sn70Pb Compression Simulation

REFERENCES

[1] B.Aefaei, Y.Xing, J.Woods, J.Wolcott, P.Tumne, P.Borgesen, and E.Cotts, Elecronnic Components and Technology Conference (2008).

[2] H.F.Zou , Z.F.Zhany, Microelectronic Engineering 87 (2010) 601-609

[3] Q.K.Zhany, O.S.Zhu, Z.F. Zhang, Materials Science and Engineering A 527 (2010) 1367-1376.

[4] Karl Seeling and David Suroski, AIM, Incorporated.

[5] P.Darbandi, T.R. Bieler, F. Pourboghrat, and Tae-Kyu Lee, Journal of Electronic Materials, Vol. 42, Issue 2, (2013), pp. 201-214

[6] Andree Lee, Deep Chouduin, and K.N Subramiuman , Lead-free Solders: Materials Reliabilty for Elecrinics, First Edition. Edited by K. N. Subramanian, (2012), p. 273.

[7] P.Kumar, Z.Huang, I. Dutta, G. Subbarayan, and R. Mahajan, Lead-free Solders: Materials Reliabilty for Elecrinics, First Edition. Edited by K. N. Subramanian, (2012), p. 197.

[8] A.U.Telang and T.R.Bieler, JOM. June (2005), pp. 44-49.

[9] Qiang Xiao, Luu Nguyen, William D.Armistrong, Elecronnic Components and Technology Conference (2004), pp. 1325-1332.

[10] Thomas R. Bieler, Bite Zhou, Lauren Blair, Amir Zamir, PayamDarbandi, FarhangPourboghrat, Tae-Kyu Lee, and Kuo-Chuan Liu, J. of Elecronic Materials, Vol. 41, No. 2, 2012, pp. 283-301 .

[11] J.Gong, C.Liu, P.P.Conway, and V.V.Silberschmidt, Comput. Mater. Sci. 39, 187(2007).

[12] Thomas R. Bieler, Adwart U. Telang, Journal of Electronic Materials, December 2009, Volume 38, Issue 12, pp. 2694-2701.

[13] R.A.Lebenson and C.N. Tome, Acta Metal.. 41, 2611 (1993).

[14] A.Zamiri, T.R. Bieler, and F.Pouboghrat , J. Electron.Mater. 38, 231 (2009).

[15] A.R.Zamiri and F.Pouboghrat, Int.J. Plast 26, 731 (2010).

[16] R.Hill, J.Mech. Phys.Solids 14, 95 (1966).

[17] R.J. Asaro and A. Needleman, Acta Metall. 33, 923 (1985)

[18] J.W. Hutchison, Proc.R. Soclond. Ser. A139, 247 (1976).

[19] R. Kappor and S. Nemat-Nasser, Scripta Mater. 40, 159 (1999).

[20] Dr.ThomasSiewert, Dr. Stephen Liu, Dr. david R. Smith, Mr. Juan Carlos Madeni, Database for Solder Properties with Emphasis on New Lead-Free Solders. National Institute of Standard and Technology &Colorado School of Mines, February (2002).

[21] J.C.M.Li, J. Mater. Sci , Mater. Electon. , (2007)

[22] K.N. Subramanian, J.G.Lee, J. of Materials Science; Materials in Electronics, 15 (2004) 235-240.

[23] Xu Chen, De-Hua Yu, Kwang Soo Kim, Materials Science and Engineering, A 406 (2005) 86-94.

[24] Huiyang Fei, Kyle Yazzie, Nikhilesh Chawla, and Hanqing Jiang, J. of Electronic Materials, Vol. 41, No. 8, (2012).

[25] Fugain Yang and J.CM.Li , Published on line: 13 October(2006).

[26] D.R.Frear, J.W. Jang, J.K. Lin, and C.ZHANG, JOM, 53(6) (2001), pp. 28-32.

[27] R. Darveaux et al., Elecronic Components and Technology Conference (2005).

[28] B. Zhou, T.R. Bieler, T.-K.Lee, and K.-C. Liu, J.Electron. Mater.38, 2702(2009).

★★★